

## RESEARCH LETTER

10.1002/2016GL071901

## Key Points:

- The 2002  $M_w$  7.3 and 2008  $M_w$  7.4 Simeulue earthquakes are “sibling” earthquakes that resemble each other and largely overlap
- These two ruptures slipped an isolated, locked asperity within a persistent rupture barrier to great earthquakes
- The rupture terminations and seismic asperity under Simeulue may be structurally controlled by a subducting morphological high of the slab

## Supporting Information:

- Supporting Information S1
- Data Set S1
- Data Set S2
- Data Set S3
- Data Set S4

## Correspondence to:

P. M. Morgan,  
Pmorgan@ntu.edu.sg

## Citation:

Morgan, P. M., L. Feng, A. J. Meltzner, E. O. Lindsey, L. L. H. Tsang, and E. M. Hill (2017), Sibling earthquakes generated within a persistent rupture barrier on the Sunda megathrust under Simeulue Island, *Geophys. Res. Lett.*, *44*, 2159–2166, doi:10.1002/2016GL071901.

Received 9 NOV 2016

Accepted 5 FEB 2017

Accepted article online 7 FEB 2017

Published online 4 MAR 2017

©2017. The Authors.

This is an open access article under the terms of the Creative Commons Attribution-NonCommercial-NoDerivs License, which permits use and distribution in any medium, provided the original work is properly cited, the use is non-commercial and no modifications or adaptations are made.

## Sibling earthquakes generated within a persistent rupture barrier on the Sunda megathrust under Simeulue Island

Paul M. Morgan<sup>1</sup> , Lujia Feng<sup>1</sup> , Aron J. Meltzner<sup>1</sup> , Eric O. Lindsey<sup>1</sup> , Louisa L. H. Tsang<sup>1</sup> , and Emma M. Hill<sup>1,2</sup> 

<sup>1</sup>Earth Observatory of Singapore, Nanyang Technological University, Singapore, <sup>2</sup>Asian School of the Environment, Nanyang Technological University, Singapore

**Abstract** A section of the Sunda megathrust underneath Simeulue is known to persistently halt rupture propagation of great earthquakes, including those in 2004 ( $M_w$  9.2) and 2005 ( $M_w$  8.6). Yet the same section generated large earthquakes in 2002 ( $M_w$  7.3) and 2008 ( $M_w$  7.4). To date, few studies have investigated the 2002 and 2008 events, and none have satisfactorily located or explained them. Using near-field InSAR, GPS, and coral geodetic data, we find that the slip distributions of the two events are not identical but do show a close resemblance and largely overlap. We thus consider these earthquakes “siblings” that were generated by an anomalous “parent” feature of the megathrust. We suggest that this parent feature is a locked asperity surrounded by the otherwise partially creeping Simeulue section, perhaps structurally controlled by a broad morphological high on the megathrust.

### 1. Introduction

The great 2004  $M_w$  9.2 Sumatra-Andaman earthquake was generated by rupture of a continuous 1600 km long span of the Sunda megathrust, which terminated to the south under Simeulue [Meltzner *et al.*, 2006]. Three months later, the megathrust ruptured another 300 km further south, generating the great 2005  $M_w$  8.6 Nias-Simeulue earthquake; the northern end of this rupture also terminated under Simeulue [Briggs *et al.*, 2006] (Figure 1). The 2004 and 2005 events uplifted the northwestern and southeastern ends of Simeulue Island, respectively, with a pattern of uplift in the shape of a saddle [Briggs *et al.*, 2006]. In addition to halting the recent 2004 and 2005 ruptures, the section of the Sunda megathrust under Simeulue, here referred to as the Simeulue section, has arrested several other great megathrust ruptures over the past 1100 years [Meltzner *et al.*, 2012]. Thus, the Simeulue section likely acts as a persistent barrier to great earthquake ruptures [Meltzner *et al.*, 2012].

Even though the Simeulue section appears to halt the propagation of great ruptures, it does not prevent the generation of small to large earthquakes [Tilman *et al.*, 2010; Feng *et al.*, 2015]. Among those, the two largest historical events have been the 2002  $M_w$  7.3 and 2008  $M_w$  7.4 Simeulue earthquakes. Notably, these two events ruptured in between or through the terminations of the great 2004 and 2005 events (Figure 1), prompting questions of why each rupture stopped where it did.

To answer these questions, we need to precisely determine the location of slip for each of the four events. However, compared to the plethora of studies of the great 2004 and 2005 events [e.g., Chlieh *et al.*, 2007; Briggs *et al.*, 2006; Konca *et al.*, 2007], few studies have been published on these smaller but still large events. DeShon *et al.* [2005] investigated the 2002 event using only far-field seismic data, and no published studies have focused on the 2008 event. Therefore, the exact locations and slip distributions of these ruptures have remained poorly known.

In this paper, we use all available near-field geodetic data including interferometric synthetic aperture radar (InSAR), GPS, and coral uplift data to develop new slip models for the 2002 and 2008 events. We find that the two events are not identical “twins” or repeating earthquakes, but they largely overlap, resembling “siblings.” The overlapping region coincides with an isolated, locked asperity in the center of an otherwise partially creeping Simeulue section [Tsang *et al.*, 2015]. We infer that this asperity may be structurally controlled, likely by a subducting morphological high.

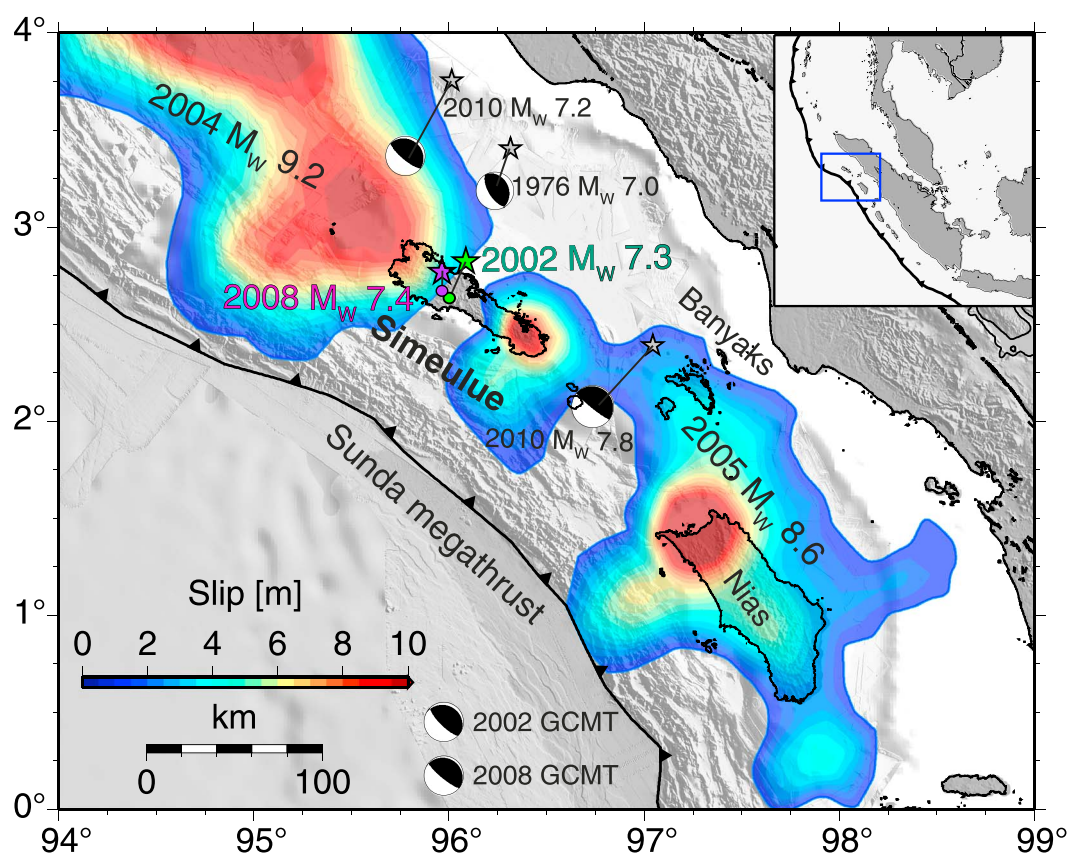


**Figure 1.** Recent  $M_w \geq 7$  earthquakes at the Simeulue section of the Sunda megathrust, offshore northern Sumatra. Stars represent epicenters from the U.S. Geological Survey (USGS) National Earthquake Information Center (NEIC) preliminary determination of epicenters (PDE) (<http://earthquake.usgs.gov/data/pde.php>). The 2002  $M_w$  7.3 epicenter is green, the 2008  $M_w$  7.4 epicenter is purple, and all others are grey. Lines connect each epicenter with the location of the corresponding focal mechanism from the global centroid moment tensor (gCMT) catalog [Ekström and Nettles, 1997; Ekström et al., 2012]. The 2002 and 2008 focal mechanisms overlap, so we plot the locations as colored circles on the map and the focal mechanisms in the legend for clarity. Closed contours indicate areas of coseismic slip ( $\geq 1$  m) for the 2004  $M_w$  9.2 Sumatra-Andaman [Chlieh et al., 2007] and the 2005  $M_w$  8.6 Nias-Simeulue [Konca et al., 2007] earthquakes. The abrupt southeastern termination of the 2004 rupture patch is likely a model artifact. The 2002 and 2008 Simeulue events occurred under central Simeulue where the 2004 and 2005 events abutted one another. Bathymetry is from Ladage et al. [2006].

In the following sections, we first describe the data, methods, and results for the more recent 2008 earthquake, because the relative wealth of geodetic data available for this event permits us to use more standard methods. We then go on to discuss the 2002 event and how the two compare.

## 2. The 2008 $M_w$ 7.4 Simeulue Earthquake

### 2.1. Data and Methods

To investigate the 2008  $M_w$  7.4 earthquake, we used ALOS-1 PALSAR images and continuous GPS data from two Sumatran GPS Array (SuGAR) stations on Simeulue Island. We processed and unwrapped the InSAR data using Generic Mapping Tools Synthetic Aperture Radar (GMTSAR) [Sandwell et al., 2011] and constructed an interferogram that spans from 4 days before to 134 days after the event (16 February 2008 to 3 July 2008) (Figure 2a). The interferogram contains the relative line-of-sight (LOS) deformation due to both coseismic and a few months of postseismic processes. Because the deformation affected the entire island, to correct the relative LOS deformation to absolute LOS deformation, we used cumulative GPS displacements during that same time period [Feng et al., 2015] (Text S1 in the supporting information). If the two GPS stations are representative of all of Simeulue, the ratios between these cumulative GPS displacements and the coseismic GPS displacements suggest that 30–40% of the signal recorded by the interferogram may be from postseismic

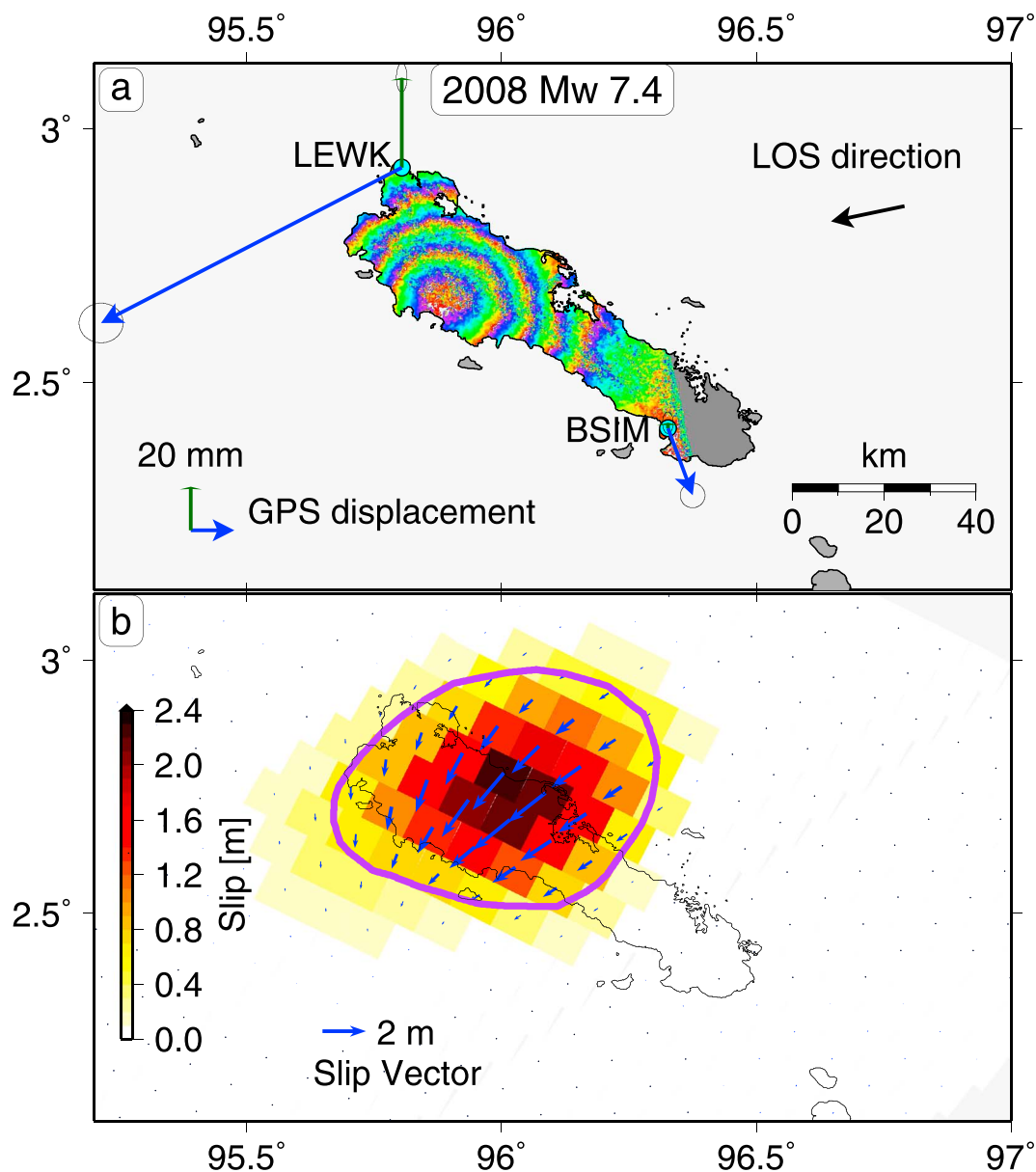


**Figure 2.** Data and model results for the 2008  $M_w$  7.4 Simeulue earthquake. (a) GPS and InSAR data used in the joint inversion. Both the GPS and InSAR data record displacements from 4 days before to 134 days after the event. For the ALOS-1 interferogram, each fringe represents 118 mm of line-of-sight (LOS) displacement with a peak LOS displacement of 624 mm. The LOS horizontal vector is shown and is  $39^\circ$  from vertical. (b) Our preferred slip inversion model for the 2008 Simeulue event. Purple line outlines the 0.5 m slip contour. Residuals are plotted in Figure S6.

processes. Then we downsampled the interferogram to 371 evenly distributed points over the island to reduce the computational burden of our inversion (Text S1).

We jointly inverted the one-dimensional InSAR observations and three-dimensional GPS observations for slip. We calculated the Green's functions using the Okada dislocation model [Okada, 1992], constrained the rake to  $90 \pm 30^\circ$ , and applied Laplacian spatial smoothing. While we tested various fault geometries (Figure S1), we chose to use a geometry based on Slab 1.0 [Hayes *et al.*, 2012]. Because the InSAR uncertainties are poorly known, we instead focused on testing different relative weightings between InSAR and GPS (Figure S2). For each relative weighting scenario, we chose a preferred slip model using a trade-off curve between data misfit and model roughness (Figure S3). Further details on the methods are given in the supporting information (Figures S4–S6).

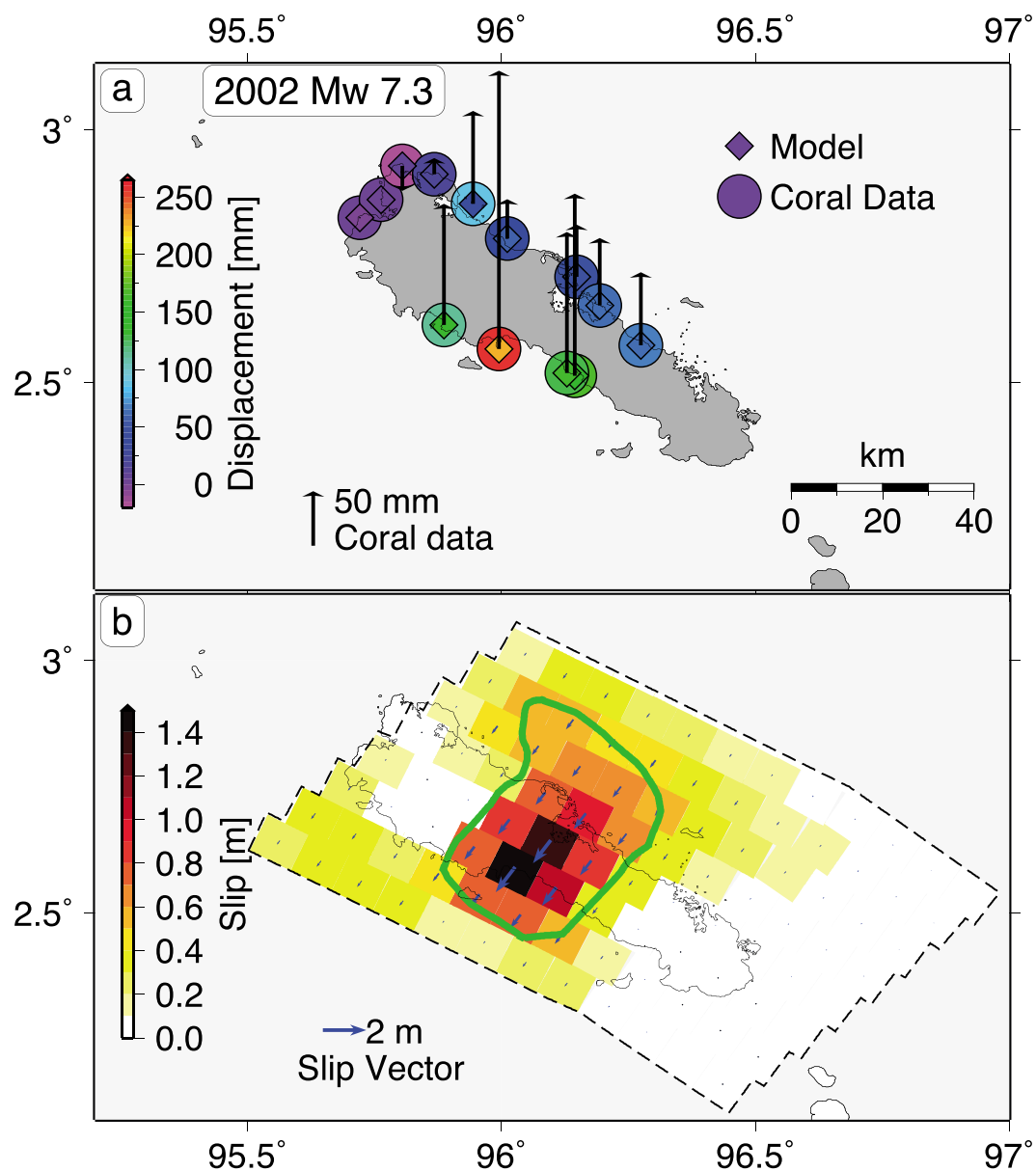


**Figure 3.** Data and model results for the 2002  $M_w$  7.3 Simeulue earthquake. (a) Coral-based observations (large circles) and model estimates (diamonds) of uplift, with the data also plotted as vectors. For clarity, uncertainties are not plotted, but they are between 80 and 100 mm ( $2\sigma$ ). (b) Our preferred slip inversion model for the 2002 Simeulue event. Green line outlines the 0.5 m slip contour. Black dashed line encloses the area that we allow to slip in the inversion.

## 2.2. Results

Figure 2b shows our preferred slip model for the 2008  $M_w$  7.4 earthquake. The slip is concentrated roughly in a circle with a diameter of  $\sim 60$  km. The maximum slip of  $\sim 2.2$  m is poorly constrained; it decreases with increasing smoothing and varies based on the depth of the slab geometry. However, tests with various slab geometries (Figure S1), weightings (Figure S2), and smoothing (Figure S3) show that the concentric circular fringes of the LOS deformation robustly constrain the location of slip to below central Simeulue.

## 3. The 2002 $M_w$ 7.3 Simeulue Earthquake

### 3.1. Data and Methods

In contrast to the wealth of data available for the 2008 event, no nearby instruments recorded the deformation from the 2002  $M_w$  7.3 event. The only geodetic data available are the vertical land motions recorded by the growth patterns of coral microatolls [Meltzner *et al.*, 2010, 2012, 2015]. Thus, we compiled a complete list of

the vertical deformation at 13 coral sites, which records the coseismic and 14 month postseismic period of the 2002 event (Figure 3a and Data Set S1). Because the coral measurements have comparatively large uncertainties, an inversion without any external constraints produced unrealistic scattered slip. Therefore, we first ran a suite of forward models to scan the megathrust and identify the bounding area (dashed lines in Figure 3b) where single patches with uniform slip could best reproduce the coral displacements (Figure S7). Within this area we then inverted for slip using a fixed rake of  $79^\circ$  from the W-phase moment tensor solution [Duputel *et al.*, 2012]. All models used the same Okada Green's functions and fault geometry as those used for the 2008 event. Further details on the methods are given in the supporting information (Figures S7–S9).

### 3.2. Results

Our preferred slip model places the slip essentially right between the slip terminations of the later 2004 and 2005 great events and directly under central Simeulue (Figure 3b). Although the position, shape, and magnitude (Text S2) of the slip patch cannot be pinpointed exactly, our forward models (Figure S7) and resolution test (Figure S9) suggest that the general location is robust. Our slip patch is updip of the one produced by DeShon *et al.* [2005], which used only far-field teleseismic waveforms. Their model overpredicts the vertical displacements at our coral sites and fails to reproduce the deformation pattern (Figure S10). The peak slip from our 2002 event model is east of that from our 2008 event model, which should be expected based on a comparison of the 2002 coral data with downscaled predictions from our 2008 model as demonstrated in Figure S11. Our results further show that coral records, even with limited precision and limited spatial and temporal resolution, can provide invaluable information about the slip of past events.

### 4. Discussion

We find that the 2002 and 2008 earthquakes were generated from slip in roughly the same area. While slightly offset, the slip distributions for those events largely overlap (Figure 4a). The similarity in location and size of these two ruptures, along with the short time span between them, is why we consider them to be sibling earthquakes, likely generated by the same parent feature of the megathrust. In the following paragraphs, we place these two ruptures in context with other known properties of the Simeulue section of the megathrust.

We first compare our slip locations with a map of coupling ratio estimated from interseismic coral subsidence rates from 1945 to 2004 [Tsang *et al.*, 2015] (Figure 4b). Broadly, the Simeulue section has a lower coupling ratio than neighboring sections, with the exception that an isolated small locked patch lies under central Simeulue. This locked patch coincides with and likely generated both the 2002 and 2008 ruptures. The high coupling ratio and repeated ruptures could be manifestations of a seismic asperity.

Next we compare our slip distributions with relatively well-located seismicity. The seismicity was recorded by a temporary seismic array deployed from late 2005 to early 2006 both on land and on the ocean floor [Tilman *et al.*, 2010]. Most of the events were concentrated within a narrow band on the slab interface (Figure 4b). The narrow seismic band roughly coincides with the updip edges of the 2002 and 2008 ruptures (this study) and the updip edge of the areas with high coupling ratios [Tsang *et al.*, 2015]. These correlations support the inference that the seismic band represents the transition zone between a shallow stable sliding zone and a deeper locked seismogenic zone [Tilman *et al.*, 2010]. The seismic band is continuous along strike except for one 20 km wide notch where the band shifts 25 km landward (Figure 4b). The landward shift in the seismic band lies at the southeastern terminations of the 2002 and 2008 ruptures.

We then explore structural features of the subducting plate that may relate to the 2002 and 2008 ruptures. In their vicinity, a broad morphological high of the slab was imaged by both 3-D tomography [Tang *et al.*, 2013] and seismic reflection [Franke *et al.*, 2008]. This morphological high could be a broad ridge with  $\sim 3$  km of relief and a width of 90 km along the strike of the trench (orange lines in Figures 4d and 4e) [Tang *et al.*, 2013]. Alternatively, the morphological high could be an asymmetric 60 km wide elevated zone with a  $\sim 1$  km ramp on its western flank and a  $\sim 3$  km ramp or tear on its eastern flank (green line in Figure 4e) [Franke *et al.*, 2008]. The broad ridge or elevated zone may result from a zone of anomalously thick oceanic crust (orange dashed line in Figure 4b) [Tang *et al.*, 2013] or the subducting fracture zone at this location [Franke *et al.*, 2008]. Although the dimensions and origin of the morphological high might be debated, its NNE–SSW trend and the location of its eastern edge are consistent in all the observations (Figure 4e). The location of the morphological high (broadly defined as between the green dashed lines in Figures 4b–4f) bounds the 2002 and 2008 ruptures and the locked patch under central Simeulue (Figures 4b and 4c).

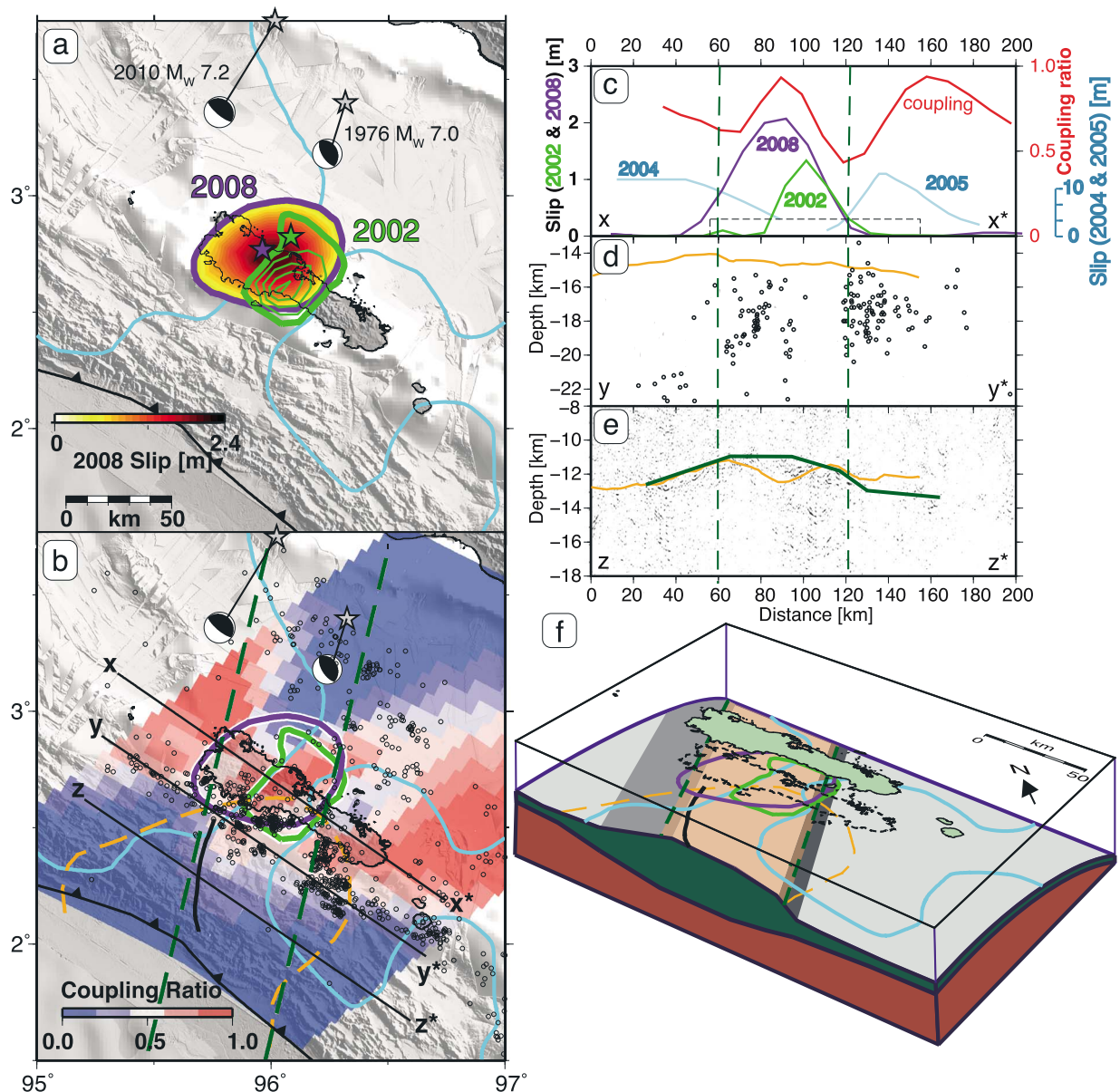


**Figure 4.** (a) The slip distributions for the 2002 and 2008 ruptures largely overlap. For 2002, green lines outline the 0.5, 0.7, 0.9, 1.1, and 1.3 m slip contours; for 2008, the purple line outlines the 0.5 m slip contour, and slip >0.5 m is indicated by the color bar. Cyan lines show the 1 m slip contour of the 2004 and 2005 ruptures. Focal mechanisms are taken from the gCMT catalog, and origins are from the USGS NEIC PDE. (b) The 2002 (green) and 2008 (purple) slip distributions placed in context with other properties of the Simeulue section. Colored patches show the estimated interseismic coupling ratio from *Tsang et al.* [2015]. Dark green dashed lines represent the edges of the segment boundary or elevated zone as proposed by *Franke et al.* [2008]. Orange dashed line indicates the extent of the subducting thick crustal zone proposed by *Tang et al.* [2013], who noted that the downdip limit of this thick crustal zone may not be well defined. Black dashed line represents the apex of the subducting ridge on the subducting plate [*Tang et al.*, 2013]. Black circles indicate seismicity located by *Tilmann et al.* [2010]. (c) Variations of slip behavior along profile  $x-x^*$ , which runs through Simeulue. The coupling profile (red), the 2004 slip profile (cyan), and the 2005 slip profile (cyan) are extracted from *Tsang et al.* [2015], *Chlieh et al.* [2007], and *Konca et al.* [2007], respectively. The 2002 and 2008 slip profiles are extracted from our preferred models. Note that the vertical scale for slip in 2004 and 2005 is different from that for slip in 2002 and 2008. Black dashed rectangle represents the location of Simeulue. (d) Orange line represents the top of the oceanic crust as defined by *Tang et al.* [2013] along profile  $y-y^*$ . Circles show the seismicity of *Tilmann et al.* [2010] within 5 km of profile  $y-y^*$ . The gap in seismicity marks the landward shift in the seismicity band. Note the depths of the top of the oceanic crust and the seismicity are all poorly constrained. (e) Orange line represents the top of the oceanic crust as defined by *Tang et al.* [2013] along profile  $z-z^*$ . The background is a vertically exaggerated seismic reflection profile BGR06-208a from *Franke et al.* [2008] with strong reflectors traced as a dark green line. (f) A vertically exaggerated schematic oblique perspective view showing the same features as those in Figure 4b. The upper depiction of Simeulue, with solid outline and fill, represents the island's location at the surface; the lower dashed outline of Simeulue, with no fill, represents the projection of Simeulue onto the megathrust interface.

Our results confirm that the 2002 and 2008 ruptures slipped in between the terminations of the great 2004 and 2005 ruptures. This location has been proposed to act as a persistent rupture barrier [Meltzner *et al.*, 2012]. To explain the barrier, several mechanisms have been suggested including (1) locally increased fluid pressure, possibly also causing the landward shift in the seismic band [Tilmann *et al.*, 2010]; (2) compositional and topographic changes associated with the subducting thick oceanic crustal zone [Tang *et al.*, 2013]; and (3) the tear on the eastern edge of the elevated zone in the subducting plate [Franke *et al.*, 2008]. Although proposed to explain the great-earthquake barrier, these mechanisms may also answer why the 2002 and 2008 ruptures stopped where they did.

We infer that the rupture terminations and the seismic asperity under Simeulue may be structurally controlled, likely by the subducting morphological high of the slab. First, the eastern edge of the morphological high seems to correlate with a poorly coupled zone under eastern-central Simeulue, which roughly matches the landward shift in seismicity, and aligns with the eastern edge of the 2002 and 2008 ruptures (Figures 4b and 4c). Second, the flat top of the morphological high is collocated with the 2002 and 2008 ruptures and the locked patch under central Simeulue (Figure 4c). Also, the down-dip projection of the morphological high may align with two other large earthquakes that occurred in June 1976 ( $M_w$  7.0) and May 2010 ( $M_w$  7.2) (Figure 4b). Third, although the western edge of the morphological high is less well defined, the western ramp proposed by Franke *et al.* [2008] may correspond to a poorly coupled zone under western Simeulue and to the western edge of the 2008 rupture (Figures 4b and 4c).

A section analogous to the Simeulue section can be found further south along the Sunda megathrust under the Batu Islands. The Batu section is estimated to be less coupled than the neighboring sections [Chlieh *et al.*, 2008] and to act as a barrier to great ruptures [Philibosian *et al.*, 2014], yet has also generated large  $M > 7$  earthquakes [Rivera *et al.*, 2002; Natawidjaja *et al.*, 2004]. This section hosts high-relief subducting structures, including the Investigator Fracture Zone [Lange *et al.*, 2010] and the Wharton fossil ridge [Henstock *et al.*, 2016]. The Investigator Fracture Zone has been suggested to control the fault coupling ratio of the section [Chlieh *et al.*, 2008], and the subducting plate morphology may relate to the asperities that ruptured in the multiple large events.

Fault morphology has only recently been recognized to play an important role in controlling megathrust ruptures [Hubbard *et al.*, 2016]. For example, the recent 2015  $M_w$  7.8 Gorkha rupture has been suggested to be controlled by ramps on the Main Himalayan Thrust [Hubbard *et al.*, 2016; Qiu *et al.*, 2016]. More specifically, earthquake cycle models show that ruptures can be terminated at local changes in gradient of a megathrust, although not consistently [Qiu *et al.*, 2016].

#### Acknowledgments

Figures were made using the Generic Mapping Tools [Wessel *et al.*, 2013]. We are grateful to the many scientists and field technicians who have spent time in rugged field conditions. These include B. Suwargadi, D. Natawidjaja, D. Prayudi, I. Suprihanto, R. Briggs, B. Philibosian, and J. Galetzka. We are grateful to Q. Qiu, K. Bradley, and S. Singh for useful discussions. We thank D. Franke and H. DeShon for sharing their results and figures for this paper. We thank P. Adamek for giving invaluable linguistic suggestions. We appreciate the Editor, J. Ritsema, one anonymous reviewer, and especially F. Tilmann, for their constructive and detailed comments that have greatly improved, and strengthened this paper. This research was supported by an NTU startup grant to E.M.H., by the National Research Foundation Singapore under its Singapore NRF Fellowship scheme (National Research Fellow Award NRF-NRFF2010-064 to E.M.H.), and by the Earth Observatory of Singapore via its funding from the National Research Foundation Singapore and the Singapore Ministry of Education under the Research Centres of Excellence initiative. This work is Earth Observatory of Singapore contribution number 138.

## 5. Conclusions

Using near-field InSAR, GPS, and coral geodetic data, we show that the slip distributions of the 2002  $M_w$  7.3 and the 2008  $M_w$  7.4 Simeulue earthquakes resemble each other and largely overlap. The closeness in location, size, and timing of these events suggests that they may be siblings generated by the same anomalous parent feature of the megathrust. The sibling ruptures coincide with a locked patch within the otherwise partially creeping Simeulue section. This coincidence could be a manifestation of a seismic asperity. The seismic asperity may be bounded within a broad morphologic high on the subduction interface. We infer that the morphological high acts as a structural control of the seismic asperity and the sibling ruptures. We also suggest that the morphological high causes the Simeulue section to act as a persistent barrier to megathrust ruptures of all sizes.

## References

- Briggs, R. W., *et al.* (2006), Deformation and slip along the Sunda megathrust in the great 2005 Nias-Simeulue earthquake, *Science*, 311(5769), 1897–1901, doi:10.1126/science.1122602.
- Chlieh, M., *et al.* (2007), Coseismic slip and afterslip of the great Mw 9.15 Sumatra-Andaman earthquake of 2004, *Bull. Seismol. Soc. Am.*, 97(1A), S152–S173, doi:10.1785/0120050631.
- Chlieh, M., J. P. Avouac, K. Sieh, D. H. Natawidjaja, and J. Galetzka (2008), Heterogeneous coupling of the Sumatran megathrust constrained by geodetic and paleogeodetic measurements, *J. Geophys. Res.*, 113, B05305, doi:10.1029/2007JB004981.
- DeShon, H. R., E. R. Engdahl, C. H. Thurber, and M. Brudzinski (2005), Constraining the boundary between the Sunda and Andaman subduction systems: Evidence from the 2002 Mw 7.3 Northern Sumatra earthquake and aftershock relocations of the 2004 and 2005 great earthquakes, *Geophys. Res. Lett.*, 32, L24307, doi:10.1029/2005GL024188.
- Duputel, Z., L. Rivera, H. Kanamori, and G. Hayes (2012), W phase source inversion for moderate to large earthquakes (1990–2010), *Geophys. J. Int.*, 189(2), 1125–1147, doi:10.1111/j.1365-246X.2012.05419.x.

- Ekström, G., and M. Nettles (1997), Calibration of the HGLP seismograph network and centroid-moment tensor analysis of significant earthquakes of 1976, *Phys. Earth Planet. Inter.*, 101(3-4), 219–243, doi:10.1016/S0031-9201(97)00002-2.
- Ekström, G., M. Nettles, and A. Dziewoński (2012), The global CMT project 2004–2010: Centroid-moment tensors for 13,017 earthquakes, *Phys. Earth Planet. Inter.*, 200–201, 1–9, doi:10.1016/j.pepi.2012.04.002.
- Feng, L., E. M. Hill, P. Banerjee, I. Hermawan, L. L. H. Tsang, D. H. Natawidjaja, B. W. Suwargadi, and K. Sieh (2015), A unified GPS-based earthquake catalog for the Sumatran plate boundary between 2002 and 2013, *J. Geophys. Res. Solid Earth*, 120, 3566–3598, doi:10.1002/2014JB011661.
- Franke, D., M. Schnabel, S. Ladage, D. R. Tappin, S. Neben, Y. S. Djajadihardja, C. Müller, H. Kopp, and C. Gaedicke (2008), The great Sumatra-Andaman earthquakes – Imaging the boundary between the ruptures of the great 2004 and 2005 earthquakes, *Earth Planet. Sci. Lett.*, 269(1–2), 118–130, doi:10.1016/j.epsl.2008.01.047.
- Hayes, G. P., D. J. Wald, and R. L. Johnson (2012), Slab1.0: A three-dimensional model of global subduction zone geometries, *J. Geophys. Res.*, 117, B01302, doi:10.1029/2011JB008524.
- Henstock, T. J., L. C. McNeill, J. M. Bull, B. J. Cook, S. P. Gulick, J. A. Austin, H. Permana, and Y. S. Djajadihardja (2016), Downgoing plate topography stopped rupture in the A.D. 2005 Sumatra earthquake, *Geology*, 44(1), 71–74, doi:10.1130/G37258.1.
- Hubbard, J., R. Almeida, A. Foster, S. N. Sapkota, P. Bürgi, and P. Tapponnier (2016), Structural segmentation controlled the 2015 Mw 7.8 Gorkha earthquake rupture in Nepal, *Geology*, 44(8), 639–642, doi:10.1130/G38077.1.
- Konca, A. O., V. Hjorleifsdottir, T.-R. A. Song, J.-P. Avouac, D. V. Helmlberger, C. Ji, K. Sieh, R. Briggs, and A. Meltzner (2007), Rupture kinematics of the 2005 Mw 8.6 Nias-Simeulue earthquake from the joint inversion of seismic and geodetic data, *Bull. Seismol. Soc. Am.*, 97(1A), S307–S322, doi:10.1785/0120050632.
- Ladage, S., C. Gaedicke, U. Barckhausen, I. Heyde, W. Weinrebe, E. R. Flueh, A. Krabbenhoef, H. Kopp, S. Fajar, and Y. Djajadihardja (2006), Bathymetric survey images structure off Sumatra, *Eos Trans. AGU*, 87(17), 165–172, doi:10.1029/2006EO170001.
- Lange, D., F. Tilmann, A. Rietbrock, R. Collings, D. H. Natawidjaja, B. W. Suwargadi, P. Barton, T. Henstock, and T. Ryberg (2010), The fine structure of the subducted Investigator Fracture Zone in western Sumatra as seen by local seismicity, *Earth Planet. Sci. Lett.*, 298(1–2), 47–56, doi:10.1016/j.epsl.2010.07.020.
- Meltzner, A. J., K. Sieh, M. Abrams, D. C. Agnew, K. W. Hudnut, J.-P. Avouac, and D. H. Natawidjaja (2006), Uplift and subsidence associated with the great Aceh-Andaman earthquake of 2004, *J. Geophys. Res.*, 111, B02407, doi:10.1029/2005JB003891.
- Meltzner, A. J., K. Sieh, H.-W. Chiang, C.-C. Shen, B. W. Suwargadi, D. H. Natawidjaja, B. E. Philipposian, R. W. Briggs, and J. Galetzka (2010), Coral evidence for earthquake recurrence and an A.D. 1390–1455 cluster at the south end of the 2004 Aceh-Andaman rupture, *J. Geophys. Res.*, 115, B10402, doi:10.1029/2010JB007499.
- Meltzner, A. J., K. Sieh, H.-W. Chiang, C.-C. Shen, B. W. Suwargadi, D. H. Natawidjaja, B. Philipposian, and R. W. Briggs (2012), Persistent termini of 2004- and 2005-like ruptures of the Sunda megathrust, *J. Geophys. Res.*, 117, B04405, doi:10.1029/2011JB008888.
- Meltzner, A. J., K. Sieh, H.-W. Chiang, C.-C. Wu, L. L. Tsang, C.-C. Shen, E. M. Hill, B. W. Suwargadi, D. H. Natawidjaja, B. Philipposian, and R. W. Briggs (2015), Time-varying interseismic strain rates and similar seismic ruptures on the Nias-Simeulue patch of the Sunda megathrust, *Quat. Sci. Rev.*, 122, 258–281, doi:10.1016/j.quascirev.2015.06.003.
- Natawidjaja, D. H., K. Sieh, S. N. Ward, H. Cheng, R. L. Edwards, J. Galetzka, and B. W. Suwargadi (2004), Paleogeodetic records of seismic and aseismic subduction from central Sumatran microatolls, Indonesia, *J. Geophys. Res.*, 109, B04306, doi:10.1029/2003JB002398.
- Okada, Y. (1992), Internal deformation due to shear and tensile faults in a half space, *Bull. Seismol. Soc. Am.*, 82(2), 1018–1040.
- Philipposian, B., K. Sieh, J.-P. Avouac, D. H. Natawidjaja, H.-W. Chiang, C.-C. Wu, H. Perfettini, C.-C. Shen, M. R. Daryono, and B. W. Suwargadi (2014), Rupture and variable coupling behavior of the Mentawai segment of the Sunda megathrust during the supercycle culmination of 1797 to 1833, *J. Geophys. Res. Solid Earth*, 119, 7258–7287, doi:10.1002/2014JB011200.
- Qiu, Q., E. M. Hill, S. Barbot, J. Hubbard, W. Feng, E. O. Lindsey, L. Feng, K. Dai, S. V. Samsonov, and P. Tapponnier (2016), The mechanism of partial rupture of a locked megathrust: The role of fault morphology, *Geology*, 44(10), 875–878, doi:10.1130/G38178.1.
- Rivera, L., K. Sieh, D. Helmlberger, and D. Natawidjaja (2002), A comparative study of the Sumatran subduction-zone earthquakes of 1935 and 1984, *Bull. Seismol. Soc. Am.*, 92(5), 1721–1736, doi:10.1785/0120010106.
- Sandwell, D., R. Mellors, X. Tong, M. Wei, and P. Wessel (2011), Open radar interferometry software for mapping surface deformation, *Eos Trans. AGU*, 92(28), 234, doi:10.1029/2011EO280002.
- Tang, G., et al. (2013), 3-D active source tomography around Simeulue Island offshore Sumatra: Thick crustal zone responsible for earthquake segment boundary, *Geophys. Res. Lett.*, 40, 48–53, doi:10.1029/2012GL054148.
- Tilmann, F. J., T. J. Craig, I. Grevemeyer, B. Suwargadi, H. Kopp, and E. Flueh (2010), The updip seismic/aseismic transition of the Sumatra megathrust illuminated by aftershocks of the 2004 Aceh-Andaman and 2005 Nias events, *Geophys. J. Int.*, 181, 1261–1274, doi:10.1111/j.1365-246X.2010.04597.x.
- Tsang, L. L. H., A. J. Meltzner, E. M. Hill, J. T. Freymueller, and K. Sieh (2015), A paleogeodetic record of variable interseismic rates and megathrust coupling at Simeulue Island, Sumatra, *Geophys. Res. Lett.*, 42, 10,585–10,594, doi:10.1002/2015GL066366.
- Wessel, P., W. H. F. Smith, R. Scharroo, J. Luis, and F. Wobbe (2013), Generic mapping tools: Improved version released, *Eos Trans. AGU*, 94(45), 409–410, doi:10.1002/2013EO450001.